Observation of Metal Transfer during Gas Metal Arc Welding

A high-speed analyzer and arc shadow-graphing system are used to better understand modes of metal transfer

BY S. RHEE AND E. KANNATEY-ASIBU, JR.

ABSTRACT. The phenomenon of metal transfer has been investigated for different transfer modes using a digital high-speed video analyzer and an arc shadow-graphing system based on a laser source and related optical system. It was observed that the pinch instability phenomenon did not occur for the globular transfer mode, since the liquid globule was then spherical rather than a cylindrical molten droplet. The drop diameters and drop transfer frequencies were measured with respect to the current for different electrode extensions and different shielding gases. On increasing the ratio of carbon dioxide to argon, the transition current from globular to spray transfer generally increased, but it is interesting that the transition was observed to occur at the lowest current in a 5% CO_2-95% argon gas mixture. This is attributed to a reduction in surface tension. For pure carbon dioxide and helium shielding gases, the drop frequency increased slowly with increasing current. At high currents for an argon-based shielding gas, the length of the molten droplet decreased as the carbon dioxide content increased because of the reaction of fume forces, which also distorted the drop shape in carbon dioxide or CO_2-argon mixture with a high carbon dioxide content. The acceleration of a droplet within the arc was determined using the gas drag force theory and was found to be greater than the experimental results.

Introduction

The International Institute of Welding (IIW) classifies metal transfer modes as globular, spray, explosive transfer in free-flight transfer, and short circuiting. The mode of metal transfer affects aspects of the welding process such as fume rate, arc stability, bead form, wetting angle and spatter. The controlling factors for the metal transfer mechanism are the welding current, wire speed, electrode extension, shielding gas, electrode polarity and wire diameter. Lesnewich (Ref. 1) investigated the metal transfer phenomenon with several parameters for mild steel. He observed that there was a sudden change in drop frequency over a narrow current range, which was called transition, and that the transition current increased with decreasing electrode extension and with increasing electrode diameter. The drop transfer frequency was measured with respect to the welding current and electrode extension using the ultraviolet oscillograph (UVO) system by Allum (Ref. 2).

It is generally known that a shielding gas is necessary to protect the electrode molten drop and weld pool from atmospheric contamination. In addition, the arc stability, metal transfer phenomenon and bead formation are strongly influenced by the shielding gas. Inert gases such as argon or helium are widely used. However, these inert gases are relatively expensive. Carbon dioxide is extensively used in gas metal arc welding since it is cheap and readily available. By reducing the surface tension, it gives good wetting characteristics. However, with the carbon dioxide shielding gas, arc and metal transfer can be unstable and spatter increases.

KEY WORDS

GMAW
Metal Transfer
Shielding Gases
Drop Frequency
Electrode Extension
Transition Current
Pinch Instability
Transfer Modes
Drop Diameters
Droplet Acceleration

In gas metal arc welding, the impact of the metal drops is known to affect the weld pool penetration (Ref. 3). Drop velocities and accelerations have been measured for the globular transfer mode over a limited current range by some authors (Refs. 4, 5). Needham, *et al.* (Ref. 6), claimed that the drop was accelerated by the plasma drag within the arc. Ma and Apps (Ref. 7) proposed that the drop velocity remained constant with time after detachment during transfer. Waszink and Piena (Ref. 8) analyzed the drop velocity and acceleration during formation, growth and necking in the pulsed current mode, assuming the square of the neck radius decreased linearly with time after the neck radius reached a critical value. Allemand, *et al.* (Ref. 9), used a He-Ne laser in conjunction with the shadow graphing technique to observe metal transfer in welding arcs.

The shielding gas effect on metal transfer is a phenomenon that is not completely understood. In this work, argon, argon-CO_2 mixtures, CO_2, and helium were used to determine the effect of shielding gas on metal transfer using a high-speed motion analyzer, and hence, the transition current and metal transfer phenomena as well as bead formation were investigated.

Experimental

The electrode used in this experiment was a mild steel welding wire (AWS A5.17) with a diameter of 1.6 mm. Pure

---

S. RHEE is a Graduate Student and E. KANNATEY-ASIBU, Jr., is an Associate Professor, Department of Mechanical Engineering and Applied Mechanics, University of Michigan, Ann Arbor, Mich.

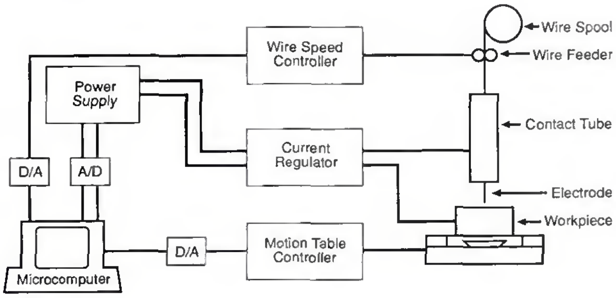

Fig. 1 — *Schematic of the welding system.*

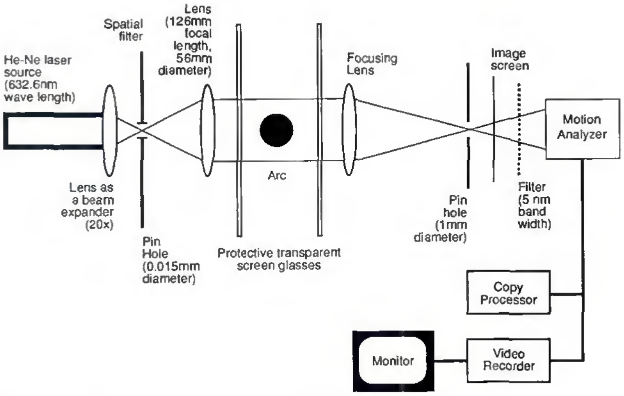

Fig. 2 — Setup of laser optics and high-speed camera system.

argon, helium, carbon dioxide and argon-CO_2 mixtures (5, 15, and 25%) were used as shielding gases. The electrode extension lengths between the contact tube and the tip of the electrode were 14, 19 and 24 mm (0.6, 0.75 and 0.9 in.). The power supply was set in the constant current mode. The wire speed and welding speed were set using a microcomputer through a digital-to-analog (D/A) converter, while the welding current was measured through an analog-to-digital (A/D) converter, using a gauge resistance of 10^{-4} ohm connected in series with the workpiece. A schematic of the welding setup is shown in Fig. 1. The metal transfer phenomenon was investigated in the constant current mode over a wide range of currents from 150 to 400 A and wire speeds from 1 to 6 m/min (3.3 to 20 ft/min), while the welding speed was 7.5 mm/s (17.7 in./s). Since a constant current power source was used, the arc voltage depended on the wire feed rate, and thus was not independently varied. However, for the conditions used, the arc voltage varied between 27 and 45 V, depending on the shielding gas and current.

To remove the high-intensity arc light, a He-Ne laser was used as a background light source along with related optical equipment. The laser source was 0.8 mm (0.03 in.) in diameter and had a wavelength of 632.6 nm with a power of 5 mW. The beam diameter was subsequently expanded 20 times after focusing the original beam at a 15-mm pinhole with a three-dimensional adjustable spatial filter. With the collimated light directed at the arc, a shadow graph of the electrode and drop was obtained. The arc light was filtered by a band pass filter of a band width 1 nm centered at 632.6 nm. To enhance the image quality, another pinhole with a 1-mm (0.04-in.) diameter was used between the final focusing lens and the image plane, onto which the image of the drop transfer was screened. The setup of laser optics and the high-speed camera system is shown in Fig. 2.

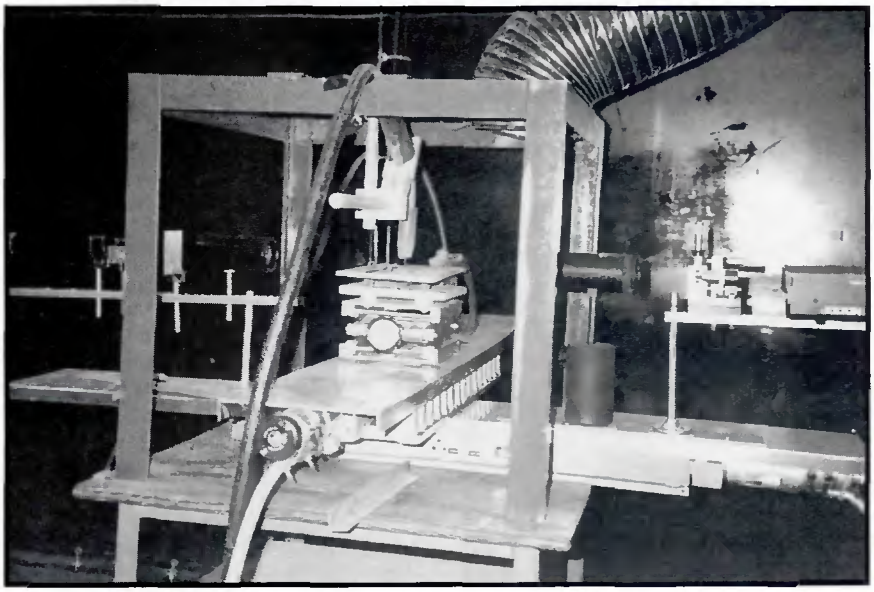

Fig. 3 — Experimental setup.

Traditionally, an ultraviolet oscillograph (UVO) has been used to measure the drop frequency by monitoring the voltage signals, and high-speed cinematographic recording has been used to pick up the images of metal transfer. Measuring the drop frequency in stream spray transfer using UVO is rather difficult and the images are not detectable. With the high-speed cinematography, it is impossible to work with real-time imaging. Furthermore, using a long film for high-speed recording can be expensive.

In this work, a high-speed video motion analyzer (Kodak Ektapro 1000) was used to acquire the image in slow motion (maximum 1000 frames/s). This frame speed is adequate for monitoring the metal transfer in all the useful current ranges. It does not have to be developed and printed. Images were obtained during welding operations that lasted ten seconds each. To adjust the electrode extension, which changes the melting rate and transfer phenomena, the current was controlled by a current knob adjustment. To measure the drop velocity and time-dependent drop formation in the high-current range, six time divisions were obtained for each frame. The drop position was determined on each picture frame using an x-y position detector. A picture of the experimental setup is shown in Fig. 3.

Results and Discussion

Drop Frequency

Typical metal transfer modes with time are shown in Fig. 4. It is very difficult to measure the drop diameter directly because of its irregularity, and, thus the drop diameters were determined indirectly from the measured drop frequency and wire speed.

Current Effect on Drop Frequency

At relatively low currents, with argon as the shielding gas, a large spherical molten metal drop was observed to be suspended at the wire tip, resulting in globular transfer. Neither a neck nor a tapering zone was observed above the molten droplet in this transfer mode — Fig. 4A. The arc then covered the lower part of the drop.

At the transition current, the drop frequency increased abruptly, as shown in Fig. 5. The arc was often found to be stable, and the drop transfer to be regular, in this region. When the current increased above the transition current, the transfer mode changed to spray transfer. In this work, the pinch instability phenomenon was only observed for the spray transfer mode, as shown in Fig. 4B.

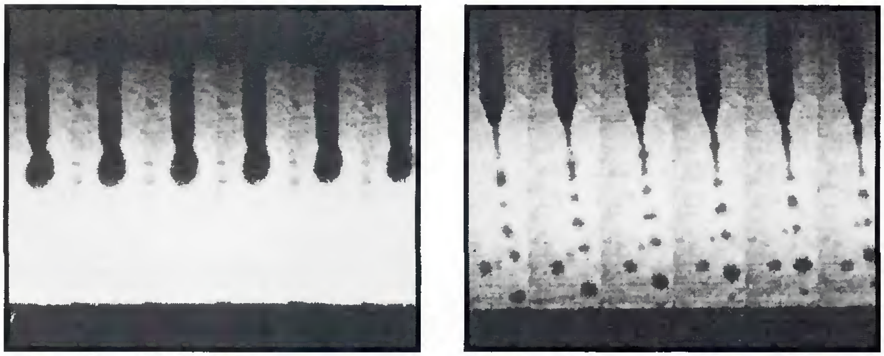

Fig. 4 — Typical metal transfer modes. Left — globular transfer; right — spray transfer.

Shielding Gas Effect on Drop Frequency

Shielding gas is used not only to protect the molten drop and the bead, but also to influence metal transfer. With carbon dioxide gas, the metal transfer mode, for the range of welding conditions investigated in this paper, is normally globular and there is no transition to spray transfer. The drop frequency was found to be between 4 and 8 drops per second up to a current of 350 A, as seen in Fig. 5. The drop was often repelled by the electromagnetic force and fume force due to vaporization of alloying elements and their oxides, resulting in spatter. The metal transfer for the helium gas was observed to be similar to that for carbon dioxide. The arc does not easily cover the entire droplet when using helium gas, probably as a result of its relatively high ionization energy. Even though the carbon dioxide gas does not have as high an ionization energy as helium, it also does not easily transfer in the spray mode even at high currents, probably because dissociation energy is required in this case also. The drop frequency that results while using helium gas is slightly higher than that for carbon dioxide. The arc root was found to be higher in argon gas, which has a low-ionization potential. However, the rationale behind the relationship between the arc root location and ionization potential of the shielding gas is not apparent at present. With pure argon, the drop frequency was observed to be much higher than that for either carbon dioxide or helium, and this may be due to its lower ionization potential. With the resulting conduction angle (*i.e.*, the angle between the electrode axis and the radius to the point at which the arc contacts the droplet) being larger for argon, the electromagnetic force is then higher for the same welding conditions. Transition from globular to spray transfer occurred at around 280 A. At current values much higher than the transition currents, the stream break-up length was long and moved sideways. Sometimes several drops were detached simultaneously by the pinch force, resulting in an irregular drop transfer.

With CO_2-argon gas mixtures, the transition current increased as the carbon dioxide content increased, as shown in Fig. 5. The reason is that a high content of carbon dioxide increased the energy potential, thereby increasing the current density. However, a 5% CO_2-95% argon mixture resulted in the minimum transition current. This is because the reduction in surface tension due to oxidation (Ref. 10) by carbon dioxide is then greater than the increase in fume force (vapor pressure) as a result of the increased oxygen content. Thus, it is easier to obtain spray transfer at lower currents when a 5% CO_2-95% argon mixture is used. As an example, when the wire feed speed was 3.4 m/min (11 ft/min), the extension length was 14 mm, and the welding current was 272 A, the drop frequency was 91 drops per second for 5% CO_2-95% argon. For the same conditions of wire speed and electrode extension, the frequency dropped to 37 drops per second for pure argon while current increased to 276 A. The experimental error range is between ± 5%.

Electrode Extension Effect

The electrode extension also plays a significant role in the mode of metal

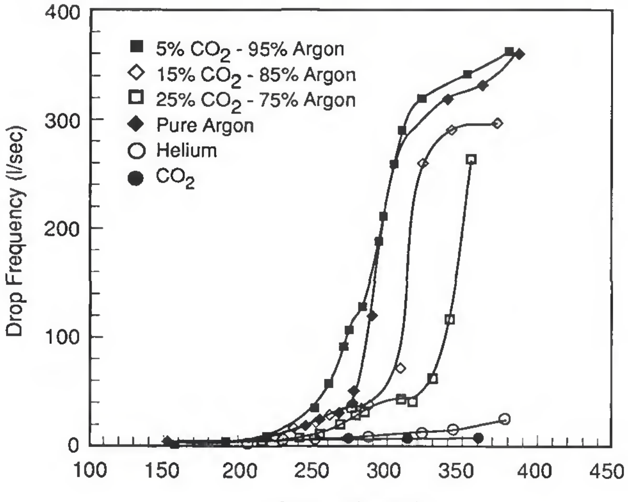

Fig. 5 — Shielding gas effect on the drop frequency.

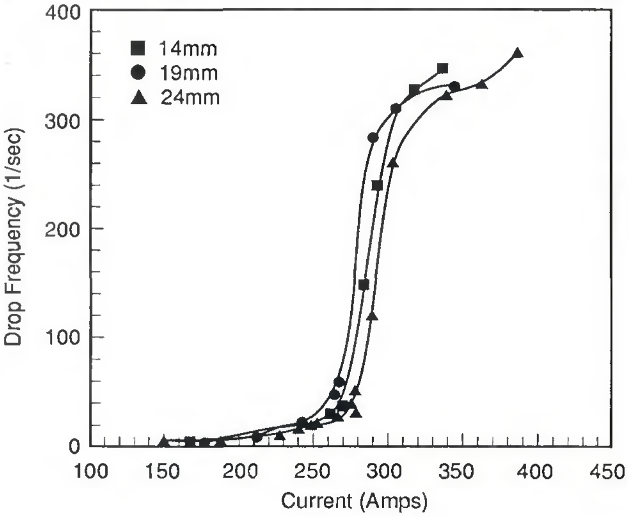

Fig. 6 — Electrode extension effect on drop frequency.

Fig. 7 — Shape of molten droplet for different shielding gases. Left — argon; center — CO_2; right — helium.

transfer. The transition current is known to be reduced as the electrode extension increases, as seen in Fig. 6. This is because when the electrode extension increases, the accompanying increase in Joule heating weakens the boundary between the liquid drop and the solid tip, resulting in an increase in the drop frequency. It was observed that the electrode extension effect is small for globular and spray transfer, but it is dominant in the transition current region.

Stability, Fumes and Bead Formation

The shape of the molten droplet as it is attached to the electrode tip depends on the shielding gas, as seen in Fig. 7. The drops in a carbon dioxide or helium atmosphere are repelled by the high current density under the drop, but the drops in argon or argon-based mixtures are more spherical with a low current density.

The cylindrical molten drop in spray transfer results in pinch instability, as seen in Fig. 4B. The forms of spray transfer for different shielding gases (argon, argon-CO_2 mixtures) are shown in Fig. 8, which shows that the break-up length becomes shorter as the carbon dioxide content increases. However, the drop frequency does not necessarily increase accordingly. In fact, it decreases with an increase in the carbon dioxide content, and that is because the drop size increases with the carbon dioxide content. Watanabe, *et al.* (Ref. 11), suggested that the fume was from the vaporization of oxides produced at the electrode tip and weld bead into the arc column. The increase in the resulting repelling force due to the fume vaporization as the carbon dioxide composition increases causes a reduction in the break-up length.

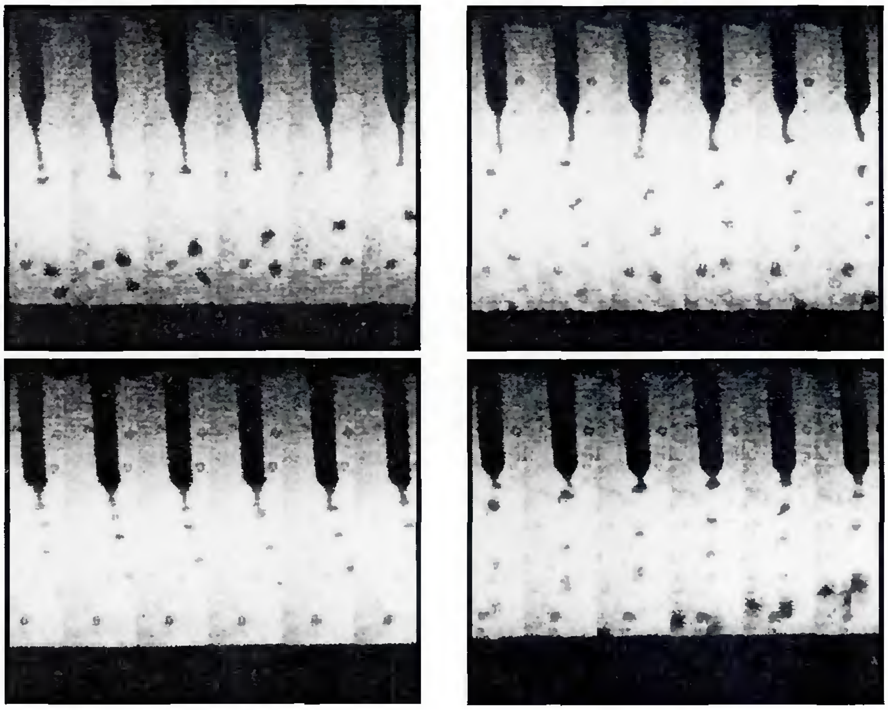

Fig. 8 — Break-up length for spray transfer.

Even though argon is an inert gas, it sometimes results in an unstable arc and produces poor bead form as metal drops explode. The pinch instability disturbances make the molten cylindrical droplet grow and separate into several droplets simultaneously. Furthermore, a high reinforcement or bad wetting characteristics may occur as a result of high surface tension. Surface tension of the molten drop and molten pool decreases with surface oxidation, producing a better wetting angle and lower reinforcement, as well as deeper side penetration. Thus, the shielding gas composition affects the height and wetting angle of reinforcement, and metal transfer through its effect on surface tension. The wetting angle is small and the weld pool crater is large when surface tension is low.

With helium gas, metal transfer occurs uniformly due to its inert characteristics, but spray transfer is not easily achieved because the arc is always under the drop due to the high ionization potential of the gas. As mentioned above, the addition of small amounts of carbon dioxide to argon produces a much higher bead quality. However, very large amounts of carbon dioxide in the argon shielding gas is not desirable, because significant amounts of spatter occur, even though the wetting characteristics improve. The weld bead forms for various shielding gases are shown in Fig. 9, and it is evident that the improvement in wetting characteristics that accompanies an increase in carbon dioxide content results in a reduction in the reinforcement.

Drop Acceleration in the Arc

A drop transfers from the electrode tip to the weld pool and is accelerated by the forces acting on it. In a carbon dioxide gas or a high ratio of carbon dioxide to argon mixture, the drop does not transfer axially to the weld pool and the resulting irregularity produces spatter. Since the arc length when using helium gas is short, it is difficult to mea-

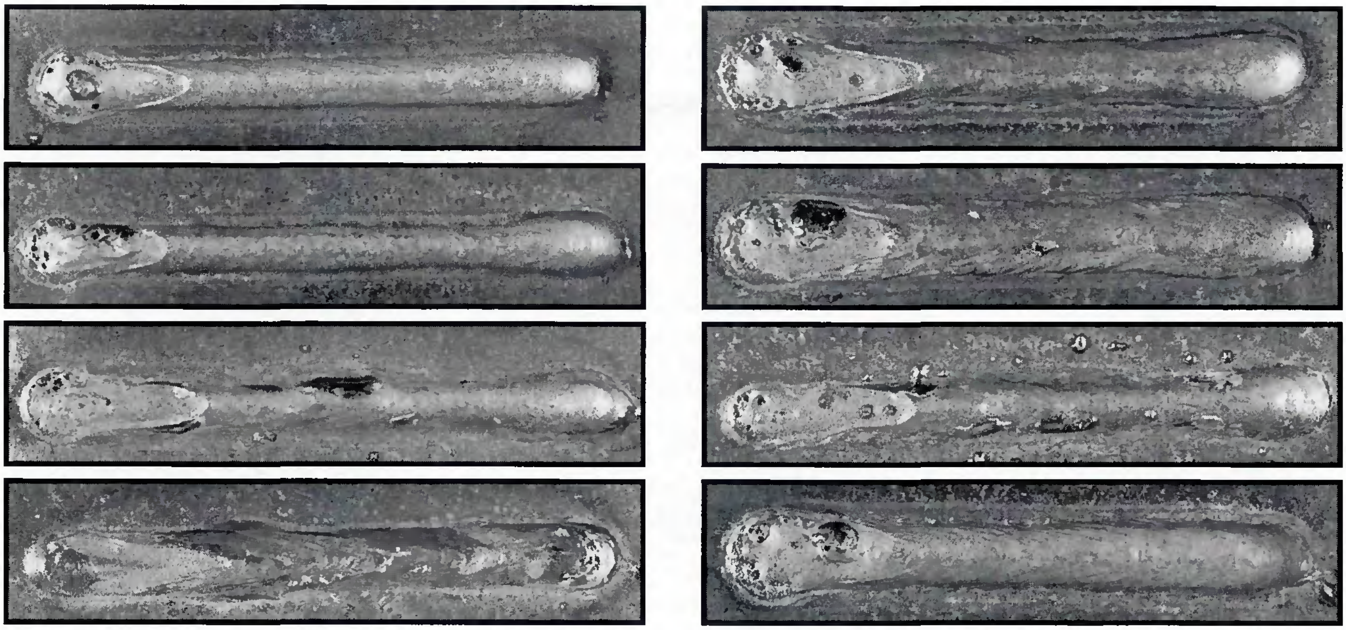

Fig. 9 — Weld bead forms for different shielding gases. Left, top to bottom — Pure argon (globular), 95% argon-5% CO_2 (globular), 85% argon-15% CO_2 (globular), CO_2; right, top to bottom — pureargon (spray), 95% argon-5% CO_2 (spray), 75% argon-25% CO_2 (spray), helium.

sure the drop motion axially when using carbon dioxide or helium shielding gas. To investigate the dynamics of metal transfer after detachment, a 5% CO_2-95% argon mixture was used.

Four different current levels were used for this experiment with a 14-mm electrode extension. The relationships between displacement and time, shown plotted in Fig. 10, were fitted with a second-order polynomial using the least squares method. The corresponding acceleration plot, shown in Fig. 11, was obtained by graphical differentiation of the displacement data. The drop acceleration was obtained by considering the plasma gas drag and was found to increase with increasing welding current by Needham, *et al.* (Ref. 6).

Conclusions

Transfer of metal during gas metal arc welding has been investigated under various welding conditions such as shielding gas, current and electrode extension using a laser-based shadowgraphing system. The transition current was found to increase as the ratio of carbon dioxide to argon ratio increased. However, it was lower in 5% CO_2-95% argon than in pure argon. Transition did not occur in either helium or carbon dioxide shielding gas. Pinch instability along the cylindrical molten droplet was observed, and the break-up stream length was found to decrease as the carbon dioxide composition increased. With the addition of carbon dioxide to argon, the height of reinforcement and wetting angle decreased as a result of a reduction in surface tension — Fig. 9. But higher contents of carbon dioxide produced spatter. The kinematics of metal transfer were determined with a high-speed motion analyzer. In 5% CO_2-95% argon, the drop acceleration was found to increase as the current increased, and the measured values are lower than the results obtained by drag theory.

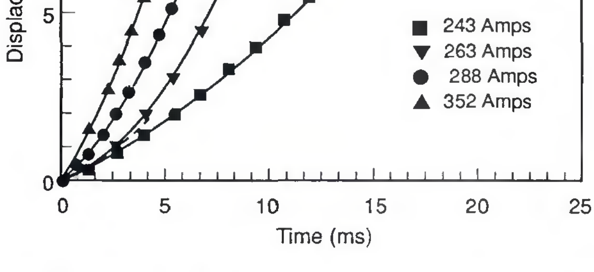

Fig. 10 — Molten drop displacement after detachment in 5% CO_2-95% argon.

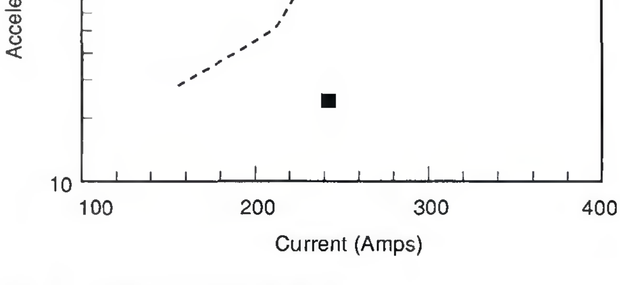

Fig. 11 — Drop acceleration within the arc.

Appendix

Nomenclature

a = acceleration of drop transfer
C_{ds} = drag coefficient for a sphere
F_d = drag force on a sphere
m = liquid drop mass
R_d = liquid drop radius
v_g = gas plasma velocity
ρ_g = gas plasma density

The drag force on a spherical drop is given by:

$$F_d = C_{ds}\frac{1}{2}\rho_g v_g^2 \pi R_d^2 \qquad (A.1)$$

where C_{ds} is the drag coefficient for a sphere and ρ_g the plasma gas density. R_d and v_g are drop radius and gas velocity, respectively. The drag coefficient for a spherical drop depends on the Reynolds number. The arc temperature for argon-iron is about 8000 K (Ref. 12), and the corresponding gas viscosity is 0.00025 kg/m-s, while the gas density is 0.06 kg/m^3 (Ref. 13). The gas velocities used are those obtained by Needham, *et al.* (Ref. 6). The velocity decreases in the radial direction, and the mean effective velocity was assumed to be half the axial value (Ref. 10). It is assumed that the acceleration is constant while a drop transfers, and that was obtained by considering the drop mass and drag force:

$$F_d + mg = ma \qquad (A.2)$$

The density of molten drop used was 7000 kg/m^3. The calculated and experimental values are compared in Fig. 11, and indicate that the measured data are much smaller than that of the calculated values, due primarily to the fume force effect, which repels the droplet, but which is not presently considered.

References

1. Lesnewich, A. 1958. Control of melting rate and metal transfer in gas shielded metal arc welding. *Welding Journal* 37(8):343-s to 353-s, 418-s to 425-s.
2. Allum, C. J. 1983. MIG welding — time for a reassessment. *Metal Construction,* Vol. 15, pp. 24–29.
3. Essers, W. G. 1981. Heat transfer and penetration mechanism with GMAW and plasma-GMAW. *Welding Journal* 60(2): 37-s to 42-s.
4. Ludwig, H. C. 1957. Metal transfer characteristics in gas-shielded arc welding. *Welding Journal* 36(1):23-s to 26-s.
5. Caron, V. 1962. Study of drop motion in the mild steel-argon arc welding system. *Canadian Metallurgical Quarterly,* Vol. 9, No. 1, pp. 373–380.
6. Needham, J. C., Cooksey, C. J., and Milner, D. R. 1960. Metal transfer in inert gas shielded arc welding. *British Welding Journal* 7(2):101–114.
7. Ma, J., and Apps, R. L. 1983. Analyzing metal transfer during MIG welding. *Welding and Metal Fabrication,* Vol. 51, pp. 119–128.
8. Waszink, J. H., and Graat, L. H. I. 1983. Experimental investigation of the forces acting on a drop of weld metal. *Welding Journal* 62(4):108-s to 116-s.
9. Allemand, C. D., Schoeder, R., Pies, D. E., and Eagar, T. W. 1985. A method of filming metal transfer in welding arcs. *Welding Journal* 64:45–47.
10. Lancaster, J. F. 1986. Metal transfer and mass flow in the weld pool. *The Physics of Welding,* 2nd. ed., Pergamon Press, New York, pp. 228–305.
11. Watanabe, I., Suzuki, M., and Kojima, T. 1979. The arc phenomena in large current MIG arc welding. *Proc. Int. conf. on Arc Physics and Weld Pool Behavior,* pp. 177–192.
12. Acinger, K. 1970. Temperature in an argon shielded welding with iron electrode. IIW Doc. 212-191-70.
13. Montain-Monval. 1973. The physical properties of fluids at elevated temperatures. IIW 212-264-73.

Recommendations Proposed by the PVRC Committee on Review of ASME Nuclear Codes and Standards Approved by the PVRC Steering Committee

WRC Bulletin 370
February 1992

The ASME Board on Nuclear Codes and Standards (BNCS) determined in 1986 that an overall technical review of existing ASME nuclear codes and standards was needed. The decision to initiate this study was reinforced by many factors, but most importantly by the need to capture a pool of knowledge and "lessons learned" from the existing generation of technical experts with codes and standards background.

Project responsibility was placed with the Pressure Vessel Research Council and activity initiated in January 1988. The direction was vested in a Steering Committee which had overview of six subcommittees.

The recommendations provided by nuclear utilities and industry were combined with the independent considerations and recommendations of the PVRC Subcommittees and Steering Committees.

Publication of this document was sponsored by the Steering Committee on the Review of ASME Nuclear Codes and Standards of the Pressure Vessel Research Council. The price of WRC Bulletin 370 is $30.00 per copy, plus $5.00 for U.S. and $10.00 for overseas, postage and handling. Orders should be sent with payment to the Welding Research Council, Room 1301, 345 E. 47th St., New York, NY 10017.

WRC Bulletin 343
May 1989

Destructive Examination of PVRC Weld Specimens 202, 203 and 251J

This Bulletin contains three reports:

(1) Destructive Examination of PVRC Specimen 202 Weld Flaws by JPVRC
By Y. Saiga

(2) Destructive Examination of PVRC Nozzle Weld Specimen 203 Weld Flaws by JPVRC
By Y. Saiga

(3) Destructive Examination of PVRC Specimen 251J Weld Flaws
By S. Yukawa

The sectioning and examination of Specimens 202 and 203 were sponsored by the Nondestructive Examination Committee of the Japan Pressure Vessel Research Council. The destructive examination of Specimen 251J was performed at the General Electric Company in Schenectady, N.Y., under the sponsorship of the Subcommittee on Nondestructive Examination of Pressure Components of the Pressure Vessel Research Committee of the Welding Research Council. The price of WRC Bulletin 343 is $24.00 per copy, plus $5.00 for U.S., or $8.00 for overseas, postage and handling. Orders should be sent with payment to the Welding Research Council, Room 1301, 345 E. 47th St., New York, NY 10017.

WRC Bulletin 354
June 1990

The two papers contained in this bulletin provide definitive information concerning the elevated temperature rupture behavior of $2\frac{1}{4}$Cr-1Mo weld metals.

(1) Failure Analysis of a Service-Exposed Hot Reheat Steam Line in a Utility Steam Plant
By C. D. Lundin, K. K. Khan, D. Yang, S. Hilton and W. Zielke

(2) The Influence of Flux Composition of the Elevated Temperature Properties of Cr-Mo Submerged Arc Weldments
By J. F. Henry, F. V. Ellis and C. D. Lundin

The first paper gives a detailed metallurgical failure analysis of cracking in a longitudinally welded hot reheat pipe with 184,000 hours of operation at 1050°F. The second paper defines the role of the welding flux in submerged arc welding of $2\frac{1}{4}$Cr-1Mo steel.

Publication of this report was sponsored by the Steering and Technical Committees on Piping Systems of the Pressure Vessel Research Council of the Welding Research Council. The price of WRC Bulletin 354 is $50.00 per copy, plus $5.00 for U.S. and $10.00 for overseas postage and handling. Orders should be sent with payment to the Welding Research Council, 345 E. 47th St., Room 1301, New York, NY 10017.